Supporting Information

Seo et al. 10.1073/pnas.0910268107

SI Materials and Methods

Plasmids and Antibodies. All expression plasmids were constructed with human BBS genes in pCS2 and phCMV2 backbone with indicated tags at the N terminus. Deletion and point mutagenesis was performed using PfuUltra II Fusion HS DNA polymerase (Stratagene) and appropriate primers (Integrated DNA Technology). Primer sequences are available upon request. For RNAi of BBS6 and BBS12, we generated stable HEK293T cell lines expressing shRNAs against these genes (GIPZ shRNAmir; OpenBiosystems). Expression of *BBS10*, *CCT1*, *CCT2*, and *CCT3* was blocked by transient transfection of siRNAs (ON-TARGETplus SMARTpool; Dharmacon). For RNAi control, we used Nonsilencing GIPZ vector (OpenBiosystems) and ON-TARGETplus Non-Targeting Pool siRNAs (Dharmacon). Antibodies against BBS1, BBS2, BBS4, and BBS7 were described previously (1). Antibody for BBS6 was raised in rabbits using peptides (ILDLSYVIEDKN) conjugated to KLH. Other antibodies were purchased from the following sources: mouse monoclonal antibodies against Myc (9E10; SantaCruz), FLAG (M2; Sigma), BBS7 (2H6; Abnova), BBS8 (Q30; SantaCruz), CCT1 (2B2-D6; Abnova), CCT2 (2G6; Abnova), β-actin (AC-15; Sigma), γ-tubulin (GTU-88; Sigma), HA (F-7; SantaCruz), rabbit polyclonal antibodies against BBS10, CCT3, CCT5, CCT8 (Proteintech Group, Inc), CCT4 (Aviva Systems Bio), γ-tubulin (Sigma), and goat polyclonal antibodies against BBS7 (D-20; SantaCruz).

Cell Culture and Immunoprecipitation. HEK293T cells were grown in DMEM (Invitrogen) supplemented with 10% FBS (Invitrogen). For individual protein–protein interaction studies, cells were transfected in six-well plates with total 2 μg indicated plasmids using FuGENE HD (Roche Applied Science). After 30 h of incubation, cells were lysed in the lysis buffer (20 mM Hepes, pH 7.5, 150 mM NaCl, 2 mM EDTA, 0.5% Triton X-100) supplemented with Complete Protease Inhibitor Mixture (Roche Applied Science). Lysates were immunoprecipitated with anti-Myc, anti-FLAG, or anti-HA antibodies conjugated to agarose beads for 2 h at 4°C. Beads were washed in the lysis buffer four times, and precipitated proteins were analyzed by SDS/PAGE and Western blotting following a standard protocol. For IP of endogenous BBS proteins, untransfected cells or cells transfected with 1 μg indicated plasmids plus 9 μg stuffer DNA in one 10-cm dish were harvested. Protein extracts were incubated with anti-FLAG, anti-HA, or anti-BBS7 antibodies overnight at 4°C. Immune complexes were precipitated by Protein G agarose (Thermo Scientific). To compare interaction efficiencies in Fig. 5 and Fig. S9, immunoblot images were scanned and band intensities were quantified by using the ImageJ program (National Institutes of Health). IP efficiencies were calculated after normalization with the input amounts of both components in the lysates. Experiments were repeated two to three times, with similar results.

Purification of BBS6-BBS12–Containing Protein Complexes and MS. A stable HEK293T cell line expressing both Myc-BBS6 and FLAG-BBS12 was generated. Lysates from this cell line and parental cell line were loaded onto anti-FLAG affinity gel (M2; Sigma), and bound proteins were eluted with 3xFLAG peptide (100 μg/mL; Sigma). Eluate was loaded onto anti-Myc affinity gel (SantaCruz), and bound proteins were eluted in 2× SDS/PAGE loading buffer. Purified proteins were resolved on 4–12% NuPAGE gels (Invitrogen) and silver stained with SilverSNAP Stain for Mass Spectrometry (Thermo Scientific) following the manufacturer's instructions. Excised gel slices were submitted to the University of Iowa Proteomics Facility and analyzed with LTQ XL linear ion trap mass spectrometer (Thermo Scientific).

Tandem Affinity Purification. Constructs for tandem affinity purification of BBS5 and BBS7 were generated with N-terminal 3xFLAG tag and S tag in CS2 plasmid (FS-BBS5 and FS-BBS7, respectively). Stable HEK293T cell lines expressing these genes were established and proteins associated with BBS5 and BBS7 were tandem affinity purified using anti-FLAG and S-protein (Novagen) affinity gels. Others are same as above. Protein identities were determined by Western blotting.

Quantitative RT-PCR. Total RNA was extracted from HEK293T cells or mouse testis and eye with TRIzol Reagent (Invitrogen) following the manufacturer's instructions. A 1-μg quantity of total RNA was used for cDNA synthesis with random primers and SuperScript II reverse transcriptase (Invitrogen). Quantitative PCR was performed with iQ SYBR Green Supermix (Bio-Rad) and Mx3000P QPCR System (Stratagene). PCR was carried out in duplicate. Relative gene expression was calculated by the ΔΔCt method after normalization with RPL19. The PCR products were confirmed by melt-curve analysis and sequencing. Primer sequences are available upon request.

Size Exclusion Chromatography. For gel filtration of mouse testis and eye extracts, testes from one animal or eyes from three animals were lysed in the lysis buffer, clarified by centrifugation, concentrated by Amicon Ultra-15 (30 kDa), and loaded on a Superose-6 10/300 GL column (GE Healthcare). For gel filtration of BBS/CCT complex, proteins partially purified by anti-FLAG affinity gel were loaded onto a Superose-6 column. Elution fractions were TCA/acetone precipitated and resuspended in 2× SDS loading buffer. Equal volumes were loaded on 4–12% NuPAGE gels and analyzed by standard immunoblotting. The column was calibrated with Gel Filtration Standard (Bio-Rad).

Immunofluorescence Microscopy. ARPE-19 cells were maintained in DMEM/F12 media (Invitrogen) supplemented with 10% FBS and seeded on glass coverslips in 24-well plates. To induce ciliogenesis, cells were shifted to serum-free medium 24 h after seeding and further incubated for 48 h. Cells were fixed with methanol for 6 min at −20°C, blocked with 5% BSA and 3% normal goat serum, and decorated with indicated primary antibodies. Alexa Fluor 488 goat anti-mouse IgG (Invitrogen) and Alexa Fluor 568 goat anti-rabbit IgG (Invitrogen) were used to detect primary antibodies. Coverslips were mounted on Vecta-Shield mounting medium with DAPI (Vector Lab), and images were taken with Olympus IX71 inverted microscope.

Analysis of Zebrafish Kupffer's Vesicle and Melanosome Transport Assay. Zebrafish embryos were injected at the one to four cell stages with MOs against *cct1*, *cct2*, and *cct3* (GeneTools), which block mRNA translation or splicing, as well as the standard control MO (GeneTools). Analysis of KV and melanosome transport was performed as previously described (2, 3). The $cct2^{hi1269Tg/+}$ line, which harbors a viral insertion in the *cct2* locus, was obtained from the Zebrafish International Resource Center (ZIRC) (4) and pairwise matings were set up using standard procedures. For statistical analysis, Fisher's exact test was used for KV defect and one-way ANOVA, followed by the Tukey test, was used for melanosome transport assay. MO sequences are shown below.

cct1 MO: ACATGTTGGACTGGAGAGAAGAAT
cct2 MO: CGGAGCCATCGATAGAGACGCCATG

cct3 MO: GTCGGCCCATCATATTTGCGGCGTG
cct2 splice MO: CACACACACAGACCTGTTGATGAAG

1. Nachury MV, et al. (2007) A core complex of BBS proteins cooperates with the GTPase Rab8 to promote ciliary membrane biogenesis. *Cell* 129:1201–1213.
2. Tayeh MK, et al. (2008) Genetic interaction between Bardet-Biedl syndrome genes and implications for limb patterning. *Hum Mol Genet* 17:1956–1967.
3. Yen HJ, et al. (2006) Bardet-Biedl syndrome genes are important in retrograde intracellular trafficking and Kupffer's vesicle cilia function. *Hum Mol Genet* 15:667–677.
4. Amsterdam A, et al. (1999) A large-scale insertional mutagenesis screen in zebrafish. *Genes Dev* 13:2713–2724.

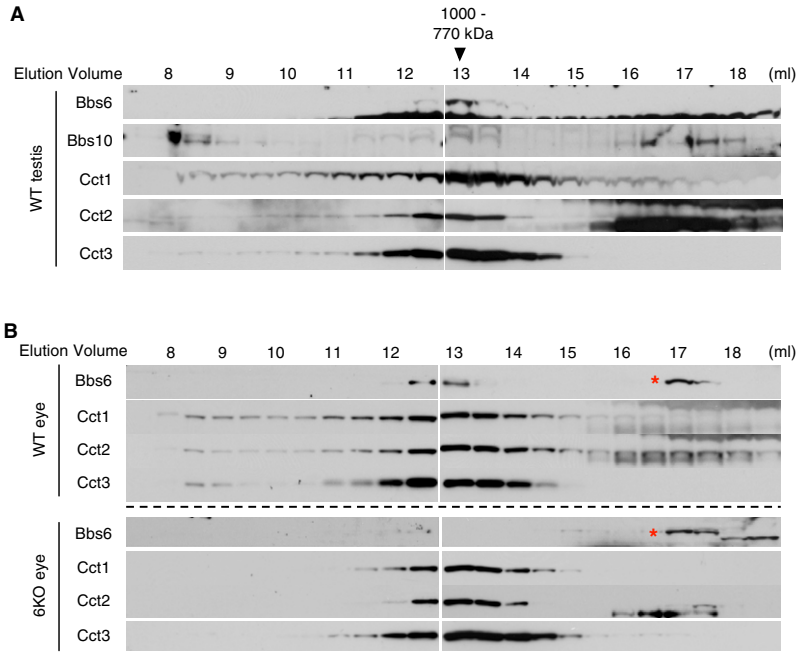

Fig. S1. Gel filtration analysis of wild-type and *Bbs6* null testis and eye extracts. Wild-type (WT) and *Bbs6* null (6KO) mouse testis (*A*) and eye (*B*) extracts were subjected to size exclusion chromatography, and elution fractions were analyzed by immunoblotting. Immunoblot result from *Bbs6* null eye extract indicates that the band ~17-mL fraction is an unknown cross-reacting protein (red asterisk). It should be noted that the Bbs6 band, present at ~13-mL fraction in wild-type, is absent in *Bbs6* null eye.

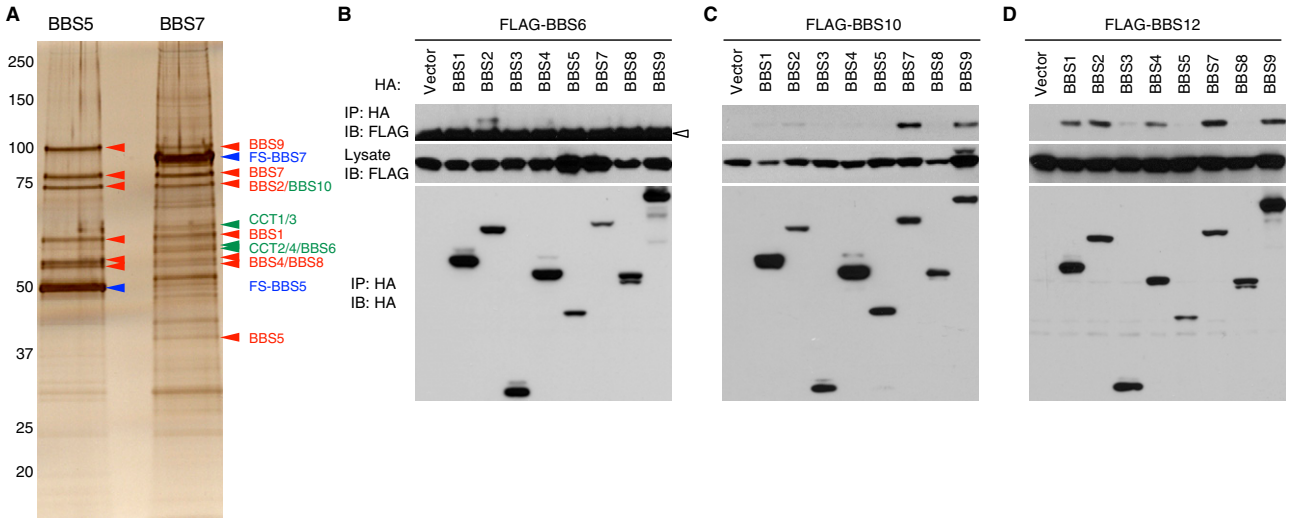

Fig. S2. Interactions between chaperonin-like BBS proteins and BBSome subunits. (*A*) The BBS/CCT complex selectively associates with BBS7. BBS5 and BBS7 were tandem affinity purified from stably transfected HEK293T cells. Although purification of BBS5 copurified only BBSome subunits (red arrowheads; BBS1, BBS2, BBS4, BBS5, BBS7, BBS8, and BBS9), purification of BBS7 resulted in copurification of the BBS/CCT complex proteins (green arrowheads; CCT1-4, BBS6, and BBS10) as well as BBSome subunits. Fusion proteins that were directly tandem affinity purified are marked with blue arrowheads. Protein identity was determined by Western blotting. It should be noted that endogenous BBS5 is absent in the FS-BBS5 sample but that endogenous BBS7 is present in FS-BBS7 sample, implying that there is only one molecule of BBS5 in the BBSome but that BBS7 may exist with different stoichiometry. (*B*) Interaction of BBS6 with BBS2. FLAG-BBS6 was cotransfected with BBSome subunits (BBS1, 2, 4, 5, 7, 8, 9) or BBS3, and lysates were subjected to IP. Input and immunoprecipitated amounts of each protein are shown. Open arrowhead marks IgG heavy chain. (*C*) Interactions of BBS10 with BBS7 and BBS9. (*D*) Interactions of BBS12 with BBS1, BBS2, BBS4, BBS7, and BBS9. Others are the same as in *B*.

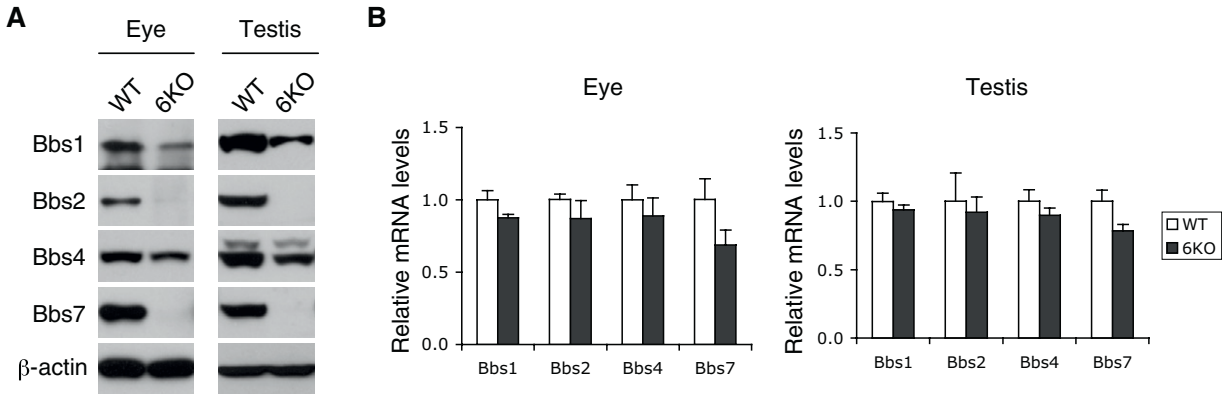

Fig. S3. Expression levels of BBS genes in *Bbs6* null mouse tissues. (*A*) Amounts of BBS proteins (Bbs1, Bbs2, Bbs4, and Bbs7) in the eye and testis. Eye and testis extracts from wild-type and *Bbs6* null mice were subjected to SDS/PAGE and immunoblotting. (*B*) Total RNA was extracted from wild-type and *Bbs6* null eye and testis, and mRNA levels of Bbs1, Bbs2, Bbs4, and Bbs7 were compared by quantitative RT-PCR. Although there was a slight decrease in BBS gene expressions in *Bbs6* null tissues, the difference was not significant.

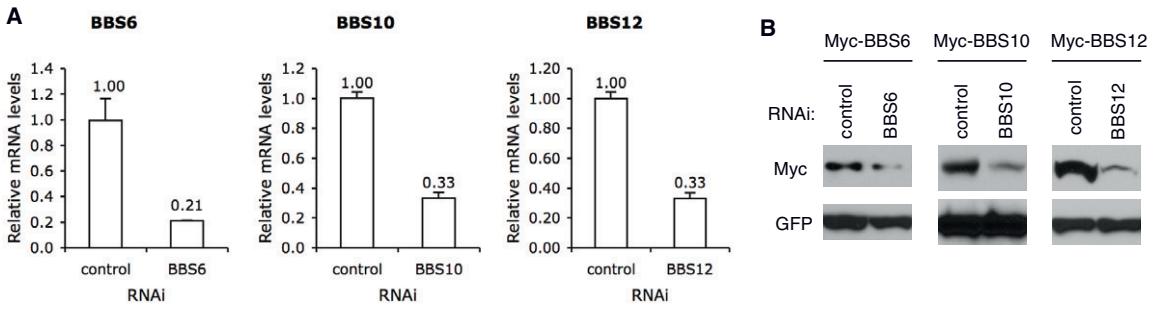

Fig. S4. Suppression of *BBS6*, *BBS10*, and *BBS12* expression in HEK293T cells. Expression of *BBS6*, *BBS10*, and *BBS12* was blocked by RNA interference (RNAi) in HEK293T cells, and the efficiency and specificity of RNAi was confirmed by quantitative RT-PCR (*A*) and immunoblotting (*B*). For quantitative RT-PCR, relative mRNA levels of endogenous BBS genes were compared after normalization with RPL19. For immunoblotting, myc-tagged expression plasmids were co-transfected with control or corresponding BBS gene siRNAs. Equal amounts of myc-GFP expression plasmids were cotransfected and used to assess transfection efficiencies and off-target effect of RNAi.

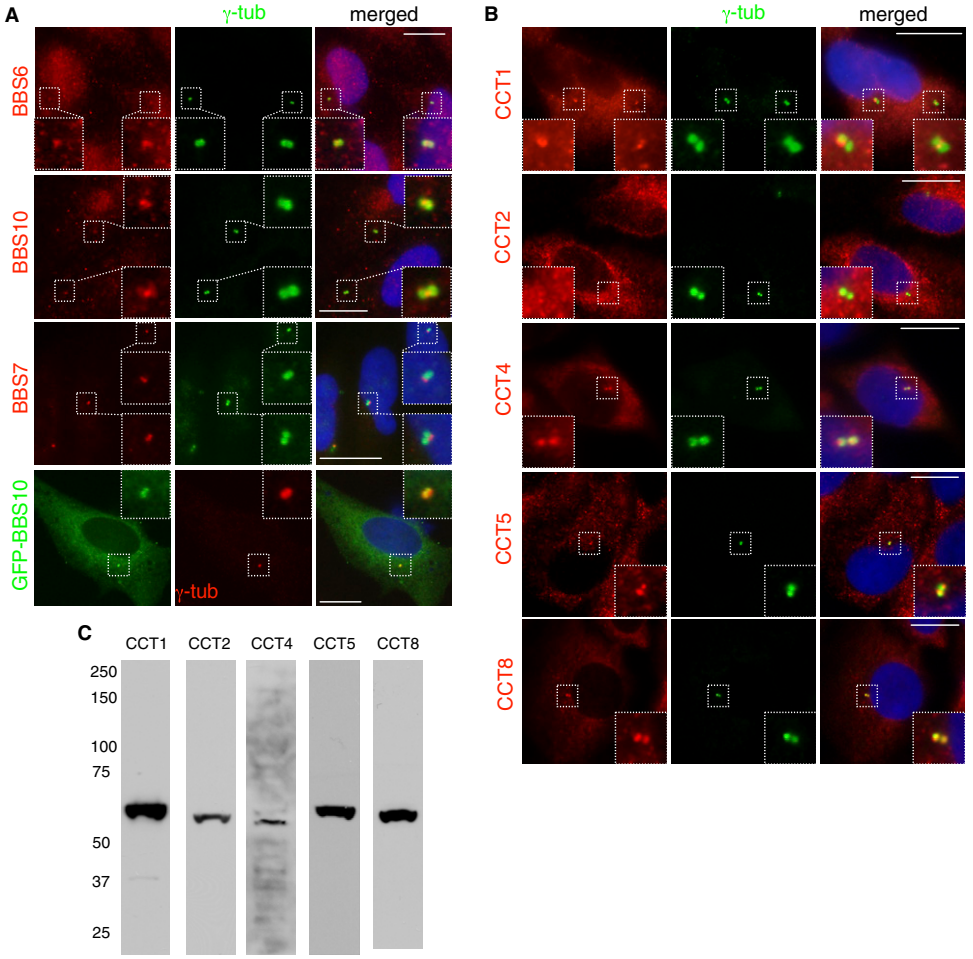

Fig. S5. Localization of chaperonin-like BBS proteins and CCT chaperonins to centrosomes. (*A*) Indirect immunofluorescence results for BBS6, BBS10, BBS7, and GFP-BBS10. (*Left*) Localization of BBS proteins. (*Center*) Location of centrosomes (γ-tubulin). (*Right*) Merged images with DAPI staining for the nucleus (blue). Inlets are enlarged images of the boxed areas around centrosomes. (Scale bars, 10 μm.) (*B*) Indirect immunofluorescence results for CCT1, CCT2, CCT4, CCT5, and CCT8. Others are the same as in *A*. (*C*) Characterization of CCT antibodies. Immunoblotting results with antibodies against CCT1, CCT2, CCT4, CCT5, and CCT8. Each antibody recognizes a single, endogenous protein with predicted molecular weights (60.3 kDa, 57.5 kDa, 57.9 kDa, 59.7 kDa, and 59.6 kDa, respectively).

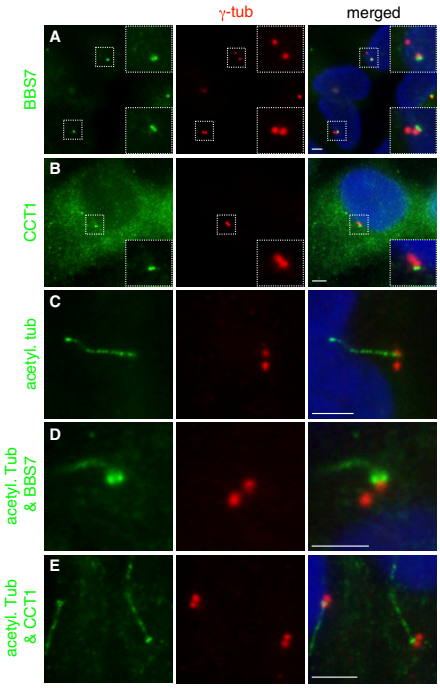

Fig. S6. BBS7 and CCT1 specifically localize to the mature centriole. BBS7 (*A*) and CCT1 (*B*) specifically localize to only one centriole of the two in ciliated ARPE-19 cells. The primary cilium (marked by acetylated tubulin in *C*) is generated from only one of the two centrioles, which is the mature or "mother" centriole and designated as the basal body. In all cases where the cilia can be unambiguously linked to one of the two centrioles, BBS7 and CCT1 staining (two green punctates in *D* and *E*) is associated with the centriole with the cilium (green whip-like structure) and within that centriole BBS7 and CCT1 are found on the side where the cilium is attached. These data indicate that BBS7 and CCT1 localize specifically to the basal body and potentially to the transition zone. However, this property does not appear to be a general feature of all BBS/CCT complex components, because we did not observe same localization in other BBS or CCT proteins tested (BBS6, BBS10, CCT4, and CCT8).

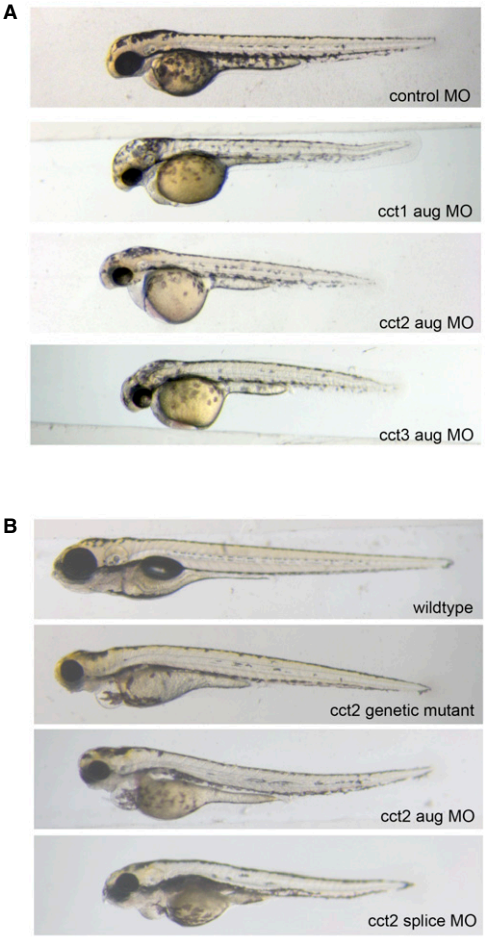

Fig. S7. Morphology of cct morphants and *cct2* mutants. Zebrafish embryos injected with indicated MOs or wild-type and *cct2* mutant embryos at 2 dpf (*A*) and 5 dpf (*B*) are shown.

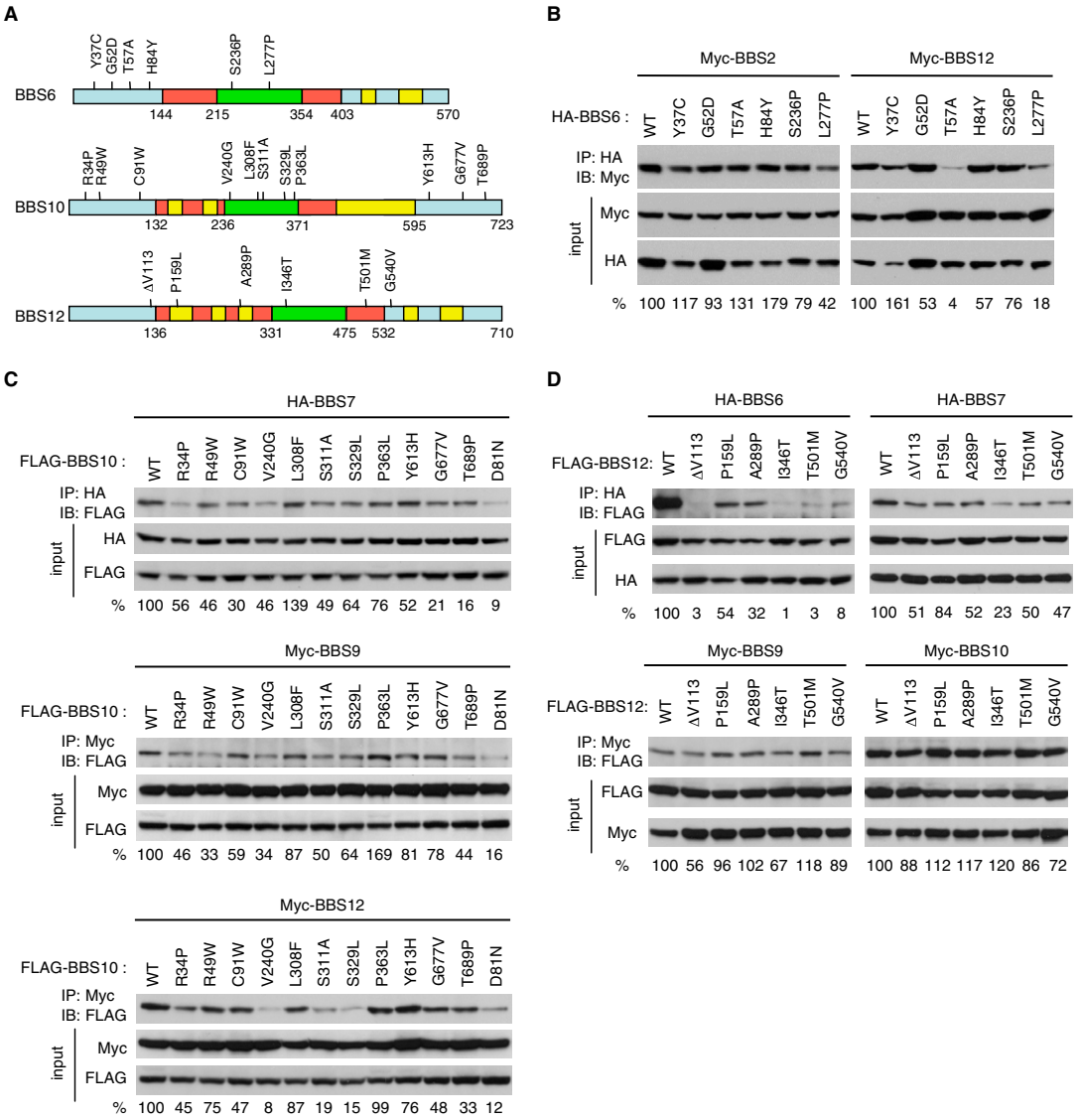

Fig. S8. Many disease-causing missense mutations found in *BBS6*, *BBS10,* and *BBS12* disrupt interactions among these proteins. (*A*) Missense mutation constructs used for interaction study. Missense mutations found in *BBS6*, *BBS10*, and *BBS12* genes in human BBS patients were depicted (17, 24, 25). Equatorial domains are in blue, intermediate domain, in red, and apical domain, in green. Yellow boxes represent insertions, which are not present in CCT family chaperonins. Numbers represent amino acid residues. (*B*) Interactions of BBS6 missense mutants with BBS2 and BBS12. HEK293T cells were transfected with Myc-BBS2 or Myc-BBS12 together with HA-BBS6 variants and lysates were subject to coimmunoprecipitation (IP) and immunoblotting (IB). Numbers at the bottom represent the ratio of coprecipitated proteins compared with wild-type protein after normalization with the input. (*C*) Interactions of BBS10 missense mutants with BBS7, BBS9, and BBS12. (*D*) Interactions of BBS12 missense mutants with BBS6, BBS7, BBS9, and BBS10. Others are same as in *B*. Note that data presented in Fig. 5 are also shown here for comparisons with other BBS proteins.

Table S1. Myc-BBS6- and FLAG-BBS12–associated proteins

Molecular weight	Name	Detected peptides	Position (aa)	Other name
80.3 kDa	BBS7	INQEMQNK	334–341	BBS2-like protein 1
		ITPVLACQDR	161–170	
		KVQLIDALK	622–630	
		LELGGVINTPQEK	69–81	
		IFIAAASEIR	82–91	
		SDNISTISILK	567–577	
		INDVICLPVER	147–157	
		LALIQITTSK	216–225	
		ESGPGEELK	325–333	
		SAVPSFGINDK	374–384	
		VQLIDALK	623–630	
60.5 kDa	CCT3	VQSGNINAAK	22–31	Chaperonin containing TCP1, subuint 3 (gamma)
		ACTILLR	333–339	
		EILSEVER	344–351	
		NLQDAMQVCR	352–361	
		AVAQALEVIPR	401–411	
		TLIQNCGASTIR	450–461	
60.3 kDa	CCT1	LGVQVVITDPEK	93–104	T-complex protein 1, TCP-1, TCP-1 alpha
		ICDDELILIK	201–210	
		TSASIILR	216–223	
		SLHDALCVVK	236–245	
		EQLAIAEFAR	279–288	
		QAGVFEPTIVK	345–355	
		VLCELADLQDK	74–84	
		YPVNSVNILK	190–199	
59.7 kDa	CCT5	LMVELSK	90–96	Chaperonin containing TCP1, subuint 5 (epsilon)
		DVDFELIK	203–210	
		FSELTAEK	345–352	
		AVTIFIR	382–388	
		QQISLATQMVR	515–525	
		MLVIEQCK	371–378	
		IADGYEQAAR	133–142	
57.9 kDa	CCT4	FSNISAAK	35–42	Chaperonin containing TCP1, subuint 4 (delta)
		GDVTITNDGATILK	66–79	
		ETLLNSATTSLNSK	161–174	
		VIDPATATSVDLR	194–206	
		VSNSGITR	233–240	
		EDIEFICK	331–338	
		LVIEEAER	396–403	
57.5 kDa	CCT2	VLVDMSR	83–89	Chaperonin containing TCP1, subuint 2 (beta)
		EAESLIAK	112–119	
		EALLSSAVDHGSDEVK	139–154	
		LAVEAVLR	182–189	
		ILIANTGMDTDK	237–248	
		GATQQILDEAER	377–388	
59.6 kDa	CCT8	DIDEVSSLLR	156–165	Chaperonin containing TCP1, subuint 8 (theta)
		TVGATALPR	327–335	
		EDGAISTIVLR	368–378	
		LATNAAVTVLR	510–520	
		AIADTGANVVVTGGK	282–296	

Table S2. Kupffer's vesicle (KV) defect and melanosome transport delay in cct morphants and *cct2* genetic mutants

	Kupffer's vesicle defect			Melanosome transport			
Treatment	*N*	KV defect (%)	*P* value	*n*	Melanosome transport (s)	SE	*P* value
Uninjected	366	3.7		65	94	1.79	
Control MO (15 ng)	92	5.4		42	99	1.22	
cct1 aug MO (5 ng)	151	26.5	0.000	40	106	3.88	NS
cct2 aug MO (15 ng)	157	18.5	0.004	22	361	19.11	<0.01
cct3 aug MO (15 ng)	157	13.4	0.054	27	117	8.78	NS
cct2 splice MO (15 ng)	96	16.7	0.019	21	171	12.10	<0.01
cct2 genetic mutant	461	1.5	0.073	27	277	16.64	<0.01
WT sibling				32	111	4.76	NS

Because *cct2* homozygotic mutants are not viable, *cct2* heterozygotes were used for mating. Embryos from this mating did not display an increase in KV defects presumably because of maternally contributed wild-type *cct2* mRNA and proteins. For statistical analysis, Fisher's exact test was used for KV assay and one-way ANOVA followed by Tukey test was used for melanosome transport assay. MO-injected groups were compared with control MO injected group, and *cct2* genetic mutants and wild-type siblings were compared with uninjected controls. NS, not significant.